Engineering and Technology Journal
Journal homepage: https://etj.uotechnology.edu.iq

Production of High-Efficiency Alternative Biodiesel from Transesterification of Waste Cooking Oil Using an In-house Made Y-Type Zeolite Catalyst

Huda A. Abdul-Kader[a], **Zaidoon M. Shakor**[a], **Bashir Y. Al-Zaidi**[a], **Shurooq T. Al-Humairi**[a]*, **Musa Salihu**[b]

[a] Chemical Engineering Dept., University of Technology-Iraq, Alsina'a street, 10066 Baghdad, Iraq.
[b] Materials Science and Engineering Dept., Kwara State University,Malete, PMB 1530, Ilorin, Kwara State Nigeria
*Corresponding author Email: shurooq.t.ramadhan@uotechnology.edu.iq

HIGHLIGHTS

- HY-zeolite catalyst was prepared from colloidal silica suspended in water by the hydrothermal method.
- Environmentally harmful waste cooking oil transesterified into biodiesel using both unloaded catalyst and KOH loaded catalyst.
- The compositions of produced biodiesel were compared with those of standard fuel and found to be almost comparable.
- The cost was significantly reduced by means of separating the spent solid HY catalyst at the end of the reaction and reactivating it for further use in post-reactions.

ARTICLE INFO

Handling editor: Qusay F. Alsalhy

Keywords:
Heterogeneous catalyst
KOH-loaded
Transesterification
Cooking oil
Biodiesel
Economic process

ABSTRACT

Y-zeolite catalyst, with a Si/Al ratio of 2.23 and a high surface area of 703.34 m^2/g_{cat}, was prepared with three different particle sizes: 75, 600, and 1000 µm, from commercial Ludox AS-40 colloidal silica 40 wt.% suspension in water using the hydrothermal method. Field Emission Scanning Electron Microscopy (FESEM), Energy Dispersive X-ray (EDX), Atomic Force Microscopy (AFM), X-ray Diffraction (XRD), Fourier Transform Infrared Spectroscopy (FTIR), and Brunauer-Emmett-Teller (BET) analyses were all utilized to analyze the properties of the synthesized Y-zeolite catalyst. Waste cooking oil (WCO) was transesterified to biodiesel in a batch reactor under different temperatures (e.g., 40, 50, and 60℃) for 3 hours, and the activity of the catalyst was evaluated before and after being loaded with potassium oxide (K_2O) molecules using the impregnation method. It is observed that the biodiesel conversion and yield, in the presence of a non-KOH-loaded catalyst, rose with increasing temperature and/or reaction time. However, increasing the reaction time beyond 2 hours in the presence of the catalyst loaded with 10% KOH decreased biodiesel conversion and yield. It has also been found that using catalysts with smaller particle sizes (e.g.,75 µm) is more favorable for enhancing the conversion of the catalytic process due to the acceleration of the reaction rate. A maximum biodiesel yield and conversion of 84.44% and 80%, respectively, were obtained. Using Gas Chromatography-Mass Spectrometry (GCMS), the composition and physical characteristics of the produced biodiesel were compared with those of standard fuels and the comparison results were particularly satisfactory. The spent Y catalyst loaded with KOH was recovered, reactivated, and reused in subsequent reactions. It exhibited outstanding catalytic activity, which is a testament to its cost advantage since it could significantly reduce the need for large quantities of costly homogeneous catalysts that are difficult to separate from the reaction products.

1. Introduction

Due to its minimal carbon monoxide emissions, biodegradability, nontoxic makeup, and lack of free sulfur, biodiesel is considered an environmentally sustainable and viable substitute. Additionally, biodiesel has been identified as a potential replacement for several characteristics of conventional diesel, such as an improved cetane number and a high flash point [1]. The feedstocks for biodiesel production are sourced from edible oils [2,3], microalgae/bacteria [4], non-edible oils [5,6], waste cooking oils [7], and animal fats such as tallow [8], yellow grease [9], lard [10], and chicken fat [11,12]. The production of biodiesel from yellow grease (waste cooking oil and animal fats) is rapidly gaining recognition as a viable solution to the two challenges currently faced by the biodiesel industry: fluctuating vegetable oil costs and the debate over whether to use the oil

http://doi.org/10.30684/etj.2023.141766.1513
Received 15 July 2023; Received in revised form 07 August 2023; Accepted 16 August 2023; Available online 14 September 2023
2412-0758/University of Technology-Iraq, Baghdad, Iraq

for food or fuel [13]. Fatty acid methyl ester (FAME) must be efficiently produced through a transesterification method that utilizes inexpensive, less corrosive, environmentally friendly, and effective catalysts. Currently, both alkaline and acidic catalysts (heterogeneous and homogeneous) are available for biodiesel synthesis. Heterogeneous catalysis is a more recent advancement in FAME synthesis than homogeneous catalysis. The use of homogeneous basic catalysts significantly accelerates the reaction rate. However, a major drawback is the high process cost due to the need to separate catalysts from the reaction medium after completion [14]. Nevertheless, several base catalysts like basic zeolites [15], alkali earth oxides [16,17], alkali earth carbonates [18], and basic hydrotalcites [19,20] have shown promising activities. Zeolites, due to their adequate pore size capable of accommodating reacting components, are the most commonly employed among various types of inorganic solids for ester formation [21]. Zeolites can be synthesized from a range of naturally occurring aluminum and silicon-based mineral compositions, as well as laboratory-synthesized silicate/alumino-silicate reagents. These components resemble those found in alumino-silicate zeolites, and examples of zeolites made from fly ash are described [22], kaolin [23], fly ash-kaolinite [24], and shale [25].

In order to produce FAME from soybean oil, W. Xie et al. utilized KOH-loaded NaX zeolite as a solid catalyst for this purpose [26]. They reported the highest yield of 85.6% under the following operating conditions: 10% KOH loading, 393 K temperature, and 3 hours reaction time. A year later, a study was conducted on converting sunflower oil to biodiesel using three types of zeolite-based catalysts: mordenite, beta, and X [27]. The impact of different loaded/stacked metals on these zeolites was examined. Zeolite X demonstrated the best performance due to its high number of super basic sites, which the other two lacked. The effect of sodium bentonite (binder) on the reactivity of these zeolites was tested, resulting in X zeolite agglomerating and causing a slight reduction in catalytic activity. Ultimately, high FAME yields of 93.5% and 95.1% were reported at 60°Cwith and without the binder, respectively.

In a related study, Wu et al. [28] attempted to produce biodiesel from soybean oil using a collection of zeolites, including NaY, KL, and NaZSM-5, loaded with CaO through microwave irradiation. A comparison was made between supported and unsupported CaO in terms of catalytic performance, with supported CaO exhibiting better performance. This was attributed to advantages conferred by the zeolite support, such as high surface area, good porosity, and strong basicity. Moreover, CaO-loaded NaY zeolite (30% doping), with a 9:1 methanol to oil (M/O) molar ratio, 3 wt.% catalyst loading, 65°C, and 3 hours reaction time, exhibited the best performance. Al-Jammal et al. [29] attempted to produce biodiesel from waste sunflower oil using the following operating conditions: 11.5:1 M/O molar ratio, 6 wt.% catalyst loading, 50°Ctemperature, and a reaction time of 2 hours. The catalysts were KOH/zeolite (1-6 M KOH), prepared by heating at 80°C for 4 hours. Manique et al. [30] once again focused on soybean oil hydrothermally converted to biodiesel using sodalite (a zeolite derived from coal) with a surface area of 10 m^2/gcat as the catalyst. A maximum FAME conversion of 95.5% was achieved under the following conditions: 12:1 M/O molar ratio, 4 wt.% catalyst loading, temperature of 65°C, and a reaction time of 2 hours.

In the present study, waste cooking oil (WCO) was converted into biodiesel using HY-zeolite catalysts prepared from colloidal silica solution as a silica source through the hydrothermal method. This type of zeolite was chosen based on its high stability and suitable pore size for the intended reaction. Using a solid catalyst aims to facilitate separation from the reaction medium after product formation, allowing for potential reactivation and reuse, thus reducing the overall industrial process cost. Various operating conditions, including reaction temperatures and times, as well as different particle sizes of the catalyst, were investigated. The primary focus of this work was exploring the particle size of the solid catalyst due to its significant effect on the reaction rate. This investigation was undertaken due to the lack of similar studies in the literature dealing with this aspect. Consequently, the optimal particle size of the solid catalyst was determined, followed by loading it with potassium hydroxide (KOH) molecules using the impregnation method and subsequent calcination at high temperatures to convert these molecules into potassium oxide (K_2O). This conversion enhances the catalytic efficiency throughout the WCO reactions. In this work, the advantage of using heterogeneous catalysts and solutions of common homogeneous catalysts in biodiesel preparation is combined.

2. Experimental Work

2.1 Materials

Colloidal Silica in the form of Ludox AS-40, a 40 wt.% suspension in water was procured from Sigma-Aldrich (USA). At the same time, granular Sodium Hydroxide (NaOH) with a purity level of 99% was supplied by CHEM-LAB (Belgium). De-ionized (DI) water with a pH of 7 and a conductivity of zero was obtained from an Iraqi manufacturer. Ammonium Chloride (NH_4Cl) was provided by the Indian company SDFCL-SD FINE-CHEM. Other raw materials used in this study, such as Sodium Aluminate ($NaAlO_2$: 50.9 wt% Al_2O_3 + 31.2 wt% Na_2O + 17.9 wt% H_2O), Sulfuric Acid H_2SO4 (98%), Pellet KOH (96.0%), and Methanol with an analytical quality of 99.5%, were all purchased from Sigma Aldrich.

Waste Cooking Oil (WCO) served as one of the primary raw materials. Cooking oil was initially collected from restaurants and homes to eliminate contaminants and food residue. The WCO was then heated to 120°C for 2 hours to remove residual moisture. The titration method was subsequently employed to determine the sample's acid amount and free fatty acid content, using Phenolphthalein as an indicator. A few drops of methanol and potassium hydroxide solution were sequentially added until the mixture turned purple. It is noteworthy that the complete chemical composition of waste cooking oil was determined using GC-MS before biodiesel production. Table 1 provides the main elements and fatty acid composition of the cooking oil. The fatty acid content of the cooking oil aligns with values reported in the published literature [31].

Table 1: Fatty acid content of waste cooking oil

No.	R.T. (min)	(Area%)	Name	Chemical Formula	FFA	M.wt.
1	20.171	6.46	Hexadecanoic acid, methyl ester (methyl palmitate)	$C_{17}H_{34}O_2$	C17:0	270
2	20.706	7.55	n-Hexadecanoic acid (palmitic acid)	$C_{16}H_{32}O_2$	C16:0	256
3	22.215	20.31	9,12-Octadecadienoic acid (Z,Z)-(linoleate acid)	$C_{19}H_{34}O_2$	C19:2	294.5
4	22.325	18.17	6-Octadecenoic acid, methyl ester	$C_{19}H_{36}O_2$	C19:1	296.5
5	22.592	8.38	Methyl stearate	$C_{19}H_{38}O_2$	C19:0	298.5
6	22.802	15.45	9,12-Octadecadienoic acid (Z,Z)-(linoleate acid)	$C_{18}H_{32}O_2$	C18:2	280.5
7	29.412	12.68	5-Heptylresorcinol	$C_{13}H_{20}O_2$	C13:0	208
8	30.959	11.06	Gamma.-Sitosterol	$C_{29}H_{50}O_2$	C29:0	414

2.2 Synthesis of NaY-Zeolite From Colloidal Silica

The Faujasite (FAU) sodium NaY-Zeolite with the chemical formula Na_{56} [Al_{56} Si_{136} O_{384}]: 250 H_2O was synthesized hydrothermally. The preparation process is outlined in the verified syntheses of the Zeolitic Materials handbook [32,33]. The seed gel was created by blending the components in precise weight compositions and allowing them to be set for approximately a day. The detailed method of preparing the seed gel includes dissolving 1g of sodium aluminate and 3.86 g of sodium hydroxide simultaneously in a plastic bottle containing deionized water. Using a pipette tube, 7.5g of Ludox AS-40 solution was added carefully to the bottle's content, and the mixture was stirred for around 10 minutes to ensure thorough mixing, utilizing a magnetic stirrer. The resulting mixture was then left to age at room temperature. The feedstock gel was prepared by mixing its constituent chemicals, which were 2.5 g of $NaAl_2O_3$, 3.29g of NaOH, and 28.04g of deionized water, in a separate plastic bottle. Accurate weights obtained from a weighing balance were used, based on calculations according to the preparation procedure. Subsequently, 18.8 g of silica suspension was added to the solution [34,35]. The resulting mixture was stirred thoroughly for 10 minutes until the white aluminosilicate gel became clear. To produce the final gel, 3.03g of the seeding gel was slowly mixed with the feedstock gel, followed by vigorous blending for twenty minutes. The resulting gel was then transferred to a Teflon bottle and heated for 18 hours in an oven set at 85℃ to ensure sufficient nucleation and crystallization times. Afterward, it was washed and filtered until a filter solution with a pH of about 8 was obtained. Following this, it was dried overnight at 110℃.

In addition, the general reaction scheme used to describe the zeolite synthesis process is as follows in Equation 1 [34]:

$$NaOH + xAl_2O_3\,.\,y\,SiO_2 \xrightarrow{(Fusion)} Na_2SiO_3 + Na_2AlO_2$$

$$NaOH_{\,(aq)} + Na_2\,Al(OH)_4(aq) + Na_2SiO_3 \xrightarrow{RoomTemperature}$$

$$\left[Na_x(AlO_2)_y(SiO_2)_z.H_2O\right]\,(gel) \rightarrow Na_p\left[(AlO_2)_p(SiO_2)_q\right]hH_2O(Crystal-in-suspension) \quad (1)$$

2.3 Preparation of HY-Zeolites

The ammonium ion exchange approach was utilized to convert the sodium form of zeolite into hydrogen (i.e., the acidic form). The ion exchange process involved mixing the laboratory-prepared solid zeolite with a 0.5 M ammonium chloride solution at 80℃ for one hour. The zeolite to ammonium chloride ratio was 1g of zeolite to 100 ml of the solution. Since removing sodium ions requires a multi-stage ion exchange technique, this procedure was repeated three times. This was done until the percentage of sodium ions within the zeolite structural framework decreased to below 0.5 wt%. It was observed that the concentration of sodium ions within the zeolite lattice decreases, resulting in an increase in the number of Na^+ ions present in the solution, as the number of ion exchange process cycles increases. The exchanged zeolite (in the ammonium form, NH_4Y) was then filtered, washed with 1L of deionized water, centrifuged for approximately 10 minutes, and subsequently dried overnight at 110 ℃. The final step was the calcination process, during which the sample was heated to 450℃ for 3 hours at an oven heating rate of 10℃/min. This step served to decompose the ammonia ions (NH_3^+) and obtain zeolite in the HY form. Figure 1 is the block diagram summarizing the method for preparing the HY zeolite from commercial Ludox AS-40.

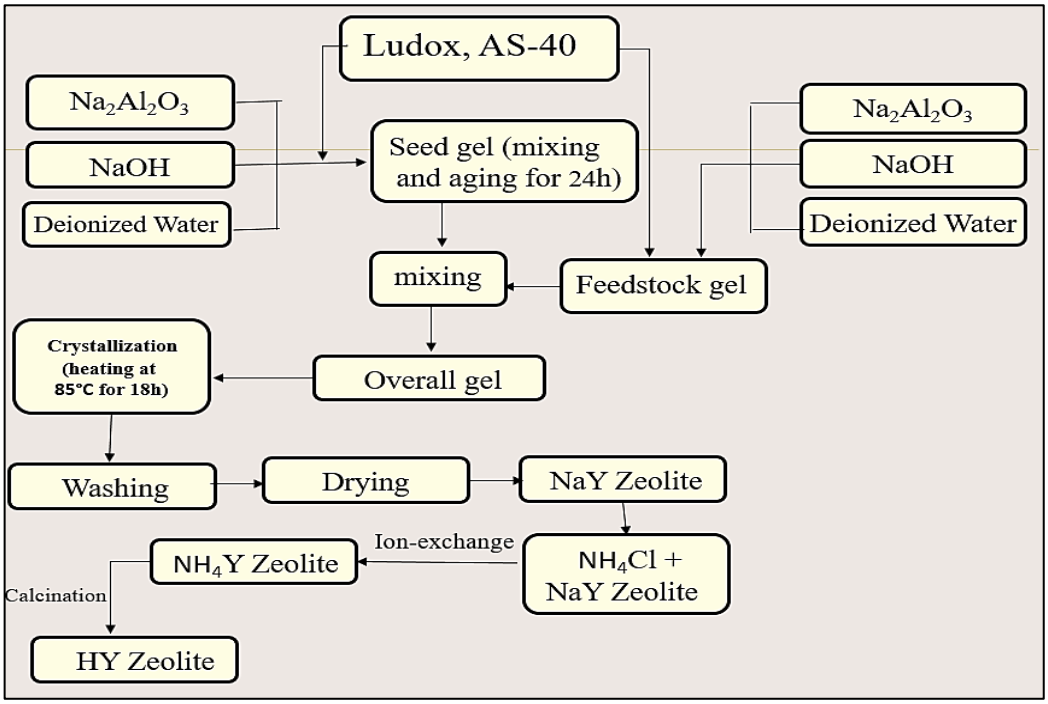

Figure 1: Block diagram for preparation HY zeolite from Ludox, AS-40

2.4 Pelletizing The Catalyst

Y-zeolite catalysts prepared as fine solid powders are not used directly in the reactor as this causes a back pressure problem. Therefore, a hydraulic press machine must be used to form these catalysts into pellets. The pressure transferred per unit area from the press to the powder is approximately 10 Tons/m^2 and was enough to produce 23 mm diameter HY-zeolite catalyst discs, weighing about 5g. The catalysts were then formed into small pellets by crushing these discs using a crusher and mortar. In order to obtain uniformly sized catalyst particles, a sieve analyzer is used to select particles with various sizes and on demand (e.g.,75, 600, and 1000 µm). Figure 2, a and b, shows Photograph of the Catalyst the catalyst discs and granular particles.

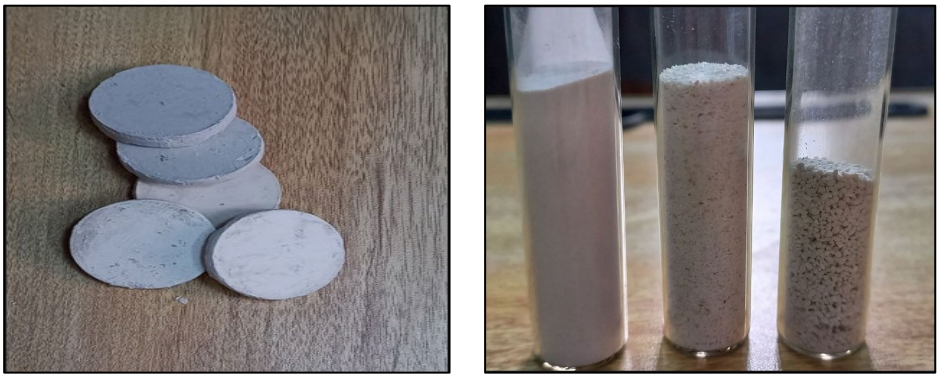

(a) Compressed catalyst disc **(b) Different sizes of catalyst particles**

Figure 2: Photograph of trhe catalyst pelletizing process

2.5 Preparation of KOH-loaded Y-Zeolite and Reactivation of The Spent Catalyst

The Y zeolite is impregnated with an aqueous solution of KOH for 24 h to ensure that the potassium hydroxide molecules diffused and distributed extensively on the surface of the Y-catalyst for the purpose of obtaining a modified Y zeolite loaded with 10 wt% KOH. The KOH molecules on the catalyst surface are then converted into potassium oxide (K_2O) form by drying the treated samples for 3 h at 125°C and followed by calcining them for 2 h at 400°C. In order to re-use the catalyst in the post-reaction, the transesterification reaction mixture is separated from the spent catalyst by centrifugation. While the final product is transported for purification, the resulting spent catalysts are reactivated by washing with cyclohexane for 2 h at 125°C, followed by drying at 105°Cto finally impregnate the catalysts with 10 wt% KOH again and become usable in subsequent reactions.

2.6 Transesterification Process

In the process of transesterification of waste cooking oil, a HY zeolite catalyst is used. The reaction is carried out in a glass reactor which is a flask with 3 necks and a circular bottom. The catalyst and alcohol are added through one side neck, which is also connected to a thermocouple. To collect the excess methanol at 64°C, which evaporates at the reaction temperature, a cooling water condenser is placed in the main reactor neck. In addition, the condenser helps maintain stable air pressure inside the reactor. The reactor is heated by an electric fabric digital heater (Type 98-1-C). Figure 3 shows the experiments performed in this system. To prepare the catalyst for use in the process, it is first dried at 130°C for 2 h to remove any moisture within it. Using a magnetic heater, 90 g of waste cooking oil is heated to the reaction temperatures before being combined with methanol and catalyst. The first reaction time determines when the reaction mixture has reached the required temperature. Different reaction parameters are studied through several sets of tests under different conditions such as temperatures (40, 50, and 60°C), catalyst pellet sizes, 75, 600, and 1000 µm, and different operational times (i.e., from 15 to 180 min). Each experiment ends with the mixing process being stopped, and the liquid chilled in an ice bath. Then the solid catalysts are separated from the mixture by centrifuging. In fact, the product is usually separated into two layers, the top layer consists of biodiesel and surplus methanol, and the bottom layer consists of glycerol. Excess methanol is removed from the resulting mixture using twice as much warm distilled water as the product. In order to separate the water and the unreacted methanol in the bottom layer from the clear biodiesel in the top layer, the batch should be left to settle and separate for about 3 h. The resulting biodiesel is extracted to determine the conversion in each batch after drying at 110°C for 10 min.

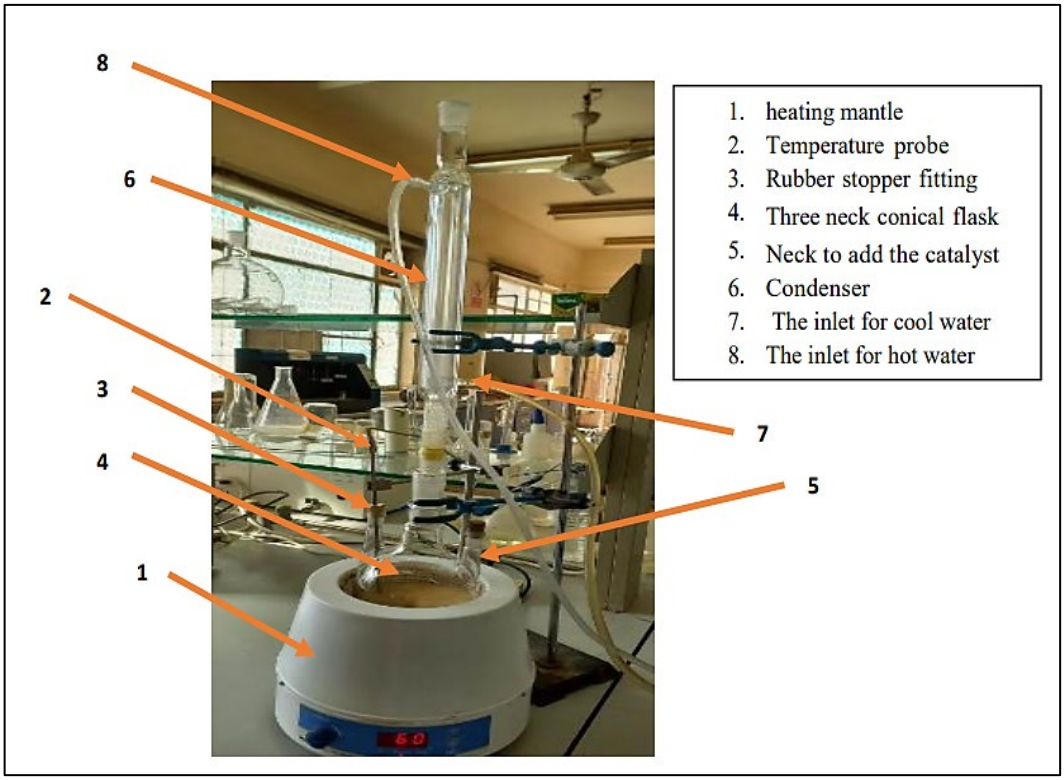

Figure 3: Experimental setup

2.7 Yield Measurement and Degree of WCO Conversion To Biodiesel

In contrast to vegetable or animal oils and fats like triglycerides, biodiesel like methyl ester dissolves readily in methanol to create a clear brilliant phase [36]. The degree of WCO conversion to biodiesel is measured using this idea. When methanol is added in a 9:1 ratio to the mixture produced from the purification phase, the conversion test can be employed successfully. After a light shake to complete the mixing process, the liquid is left to settle for 30 min. As a result, the separation funnel separates the product into two layers. The unconverted oil is found in the first bottom layer, while the methanol-methyl ester combination is found in the second layer, which is the top layer. The biodiesel fraction, which depends on the methanol/sample ratio, is transferred to methanol after the unreacted oil is drained. This is consistent with the research published previously in the literature [35,37]. The conversion percentage of WCO and biodiesel yield can be calculated using Equations 2 and 3, respectively:

$$Conversion\ \% = \frac{Initial\ weight\ of\ oil - unreacted\ \ weight\ of\ oil}{nitial\ weight\ of\ oil} \quad (2)$$

$$Yield\ \% = \frac{Product\ FAME}{nitial\ weight\ of\ oil} \quad (3)$$

3. Catalyst Characterization

3.1 XRD Analysis

To demonstrate the successful synthesis of Y-type zeolites using the hydrothermal technique, the crystal composition of the synthesized sample was obtained, as shown in the XRD pattern in Figure 4. The XRD patterns confirm that the as-synthesized Y-zeolite structure, loaded with 10 wt.% KOH, and the regenerated Y-zeolite had almost the same patterns as well as equal main peaks compared to the XRD pattern of a standard FAU zeolite described by the International Zeolite Association (IZA) [34,38]. According to the 2-Theta values in Table 2, this comparison indicates that the results of the preparation method are consistent with the crystal structure of Y zeolite, which means that the preparation method using Ludox AS-40 as a source of primary building unit(s) for the catalyst lattice succeeded remarkably. In addition, it is also noted that the process of reactivating at high temperatures for the spent catalyst, after the reaction, does not appear to affect the structure of the catalyst because the XRD pattern of the regenerated catalyst remained without a complete or partial collapse in its structural framework. The extent of crystallinity in the zeolite Y sample was computed based on the sum of intensities of the main peaks from the XRD by taking a ratio of the sum of the main peak intensities of the produced zeolite Y to that of the main peak intensities of the standard Y-zeolite. The peak intensity values are used to estimate the degree of crystallinity using Equation 4 [39], and they are approximately equal to 154.23% for the prepared NaY zeolite.

$$Degree\ of\ Crystallinity = \frac{\Sigma\ peak\ intensities\ of\ the\ synthesized\ \ zeolit-Y}{\Sigma\ peak\ intensities\ of\ the\ Reference\ \ zeolit-Y} \quad (4)$$

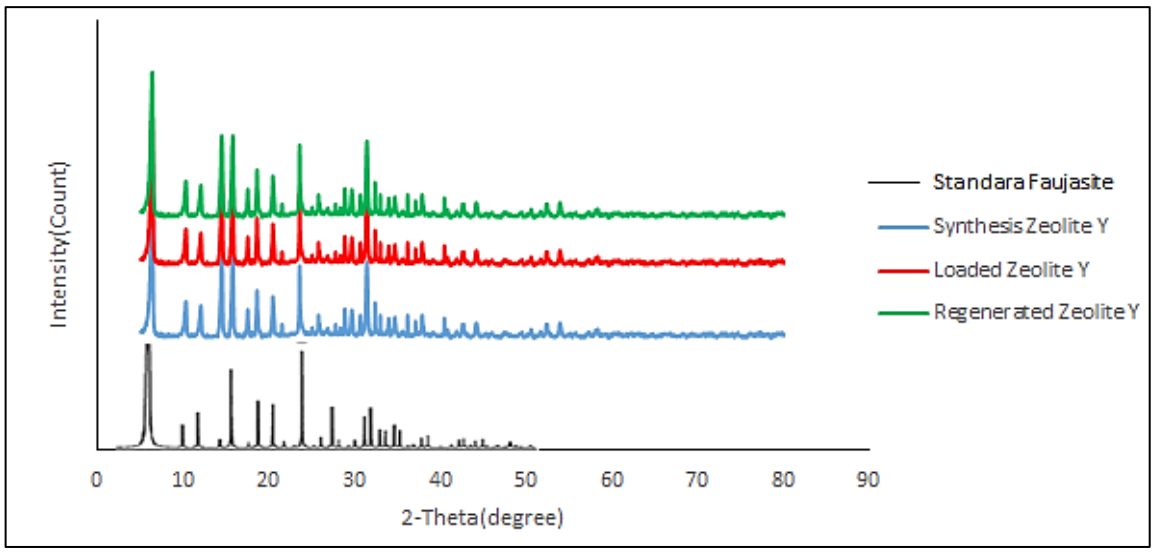

Figure 4: XRD-pattern of the synthesized zeolite Y

The table also shows the degree of crystallinity of the synthesized sample at a high level. The intensities of the peaks above the identical position of 2-Theta of the synthesized sample and the reference sample were applied in the calculations. Moreover, they confirmed the purity of the framework structures of the synthesized model. As a result, firstly, preparation is successful, and the structure is highly crystalline; secondly, the percentage is greater than 100%. This occurred due to the differences in the XRD diffractometers used, which have different manufacturing factors—resulting in a divergence in sample analysis. On the other hand, the synthesized zeolite-Y can be considered more crystalline compared with standard Faujasite.

Table 2: Comparison of the lattice spacing between the prepared NaY catalyst and the standard Faujasite

Standard Faujasite		Synthesized NaY Zeolite	
2-Theta (degree)	**Standard Faujasite intensity (I)**	**2-Theta (degree)**	**Synthesized sample intensity (I)**
6.233	100	6.23	149
15.640	53	15.64	55
20.360	38	20.40	83
23.635	59	23.64	84
27.042	39	27.04	41
30.730	22	30.72	64
31.378	49	31.36	30
32.432	16	32.40	66
34.053	15	34.04	31
Sum	391	Sum	603
Degree of crystallinity	100%	Degree of crystallinity	154.23%

3.2 Surface Area and Pore Volume

By employing the Brunauer, Emmett, and Teller technique to evaluate nitrogen adsorption at 77 K, the surface area of the produced catalyst is determined to be 703.34 $m^2/g_{-cat.}$, and the pore volume is 0.3669 cm^3/g_{-cat}. Since heterogeneous catalysis is an interface phenomenon, increasing surface area often increases the catalyst activity. Furthermore, a high surface area usually contains a high percentage of micropores, which are more hydrothermally stable than others [40]. The values of the surface area of the Y-zeolite documented by other authors are about 483.4 m^2/g_{-cat}. [41] and 244.38 m^2/g_{-cat}. [42], which are much lower compared to those obtained in the current study.

3.3 Field Emission Scanning Electron Microscopy (FE-SEM) Analysis

Figure 5 displays FSEM-images of Y-zeolite with a magnification of (a) 1000X and (b) 5000X of laboratory-synthesized zeolites. FESEM images with sizes ranging from 1,000 to 5,000 nm of samples produced using colloidal silica and sodium silicate as the silica source revealed sharp micro-shapes of the crystals of the synthesized catalyst. The figure also shows that Y-zeolite contains agglomerated crystals whose size is less than 124 nm. According to Nsaif et al. [43], at the nano-scale, the active forces are Van Der Waals and surface tension. This FSEM provides information on crystals size and distribution and how they agglomerate under the influence of these forces.

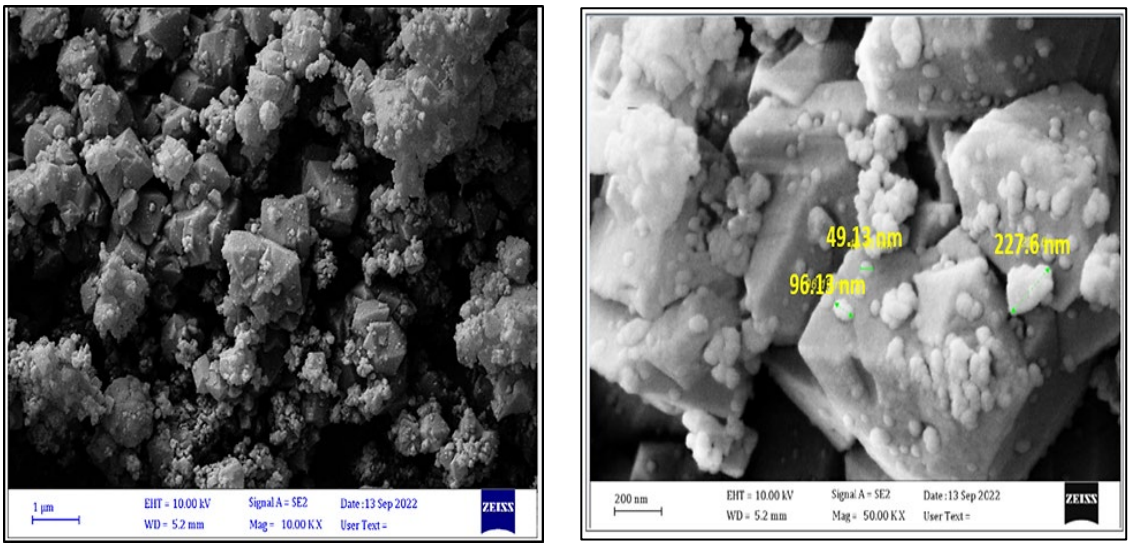

(a) Magnification 1000X **(b) Magnification 5000X**

Figure 5: FSEM-images of Y-zeolite with a magnification of (a) 1000X and (b) 5000X

3.4 Energy Dispersive X-ray (EDX) Analysis

According to the EDX results shown in Figures 6, a and b, the indicative bulk Si/Al ratio within the Y-zeolite lattice was estimated to be 2.23, which agrees well with results published by Matti et al. [44] as well as Souza et al. [45]. In order to replace the sodium ion in NaY-zeolite with ammonium to form NH_4Y, an ammonium chloride salt solution was used for the three-step ion exchange involved. After the treatment, an EDX test was conducted to determine the sodium concentration of the zeolite. The analysis reveals that the concentration decreased from 8.11 to around 0.49 wt.%, indicating successful treatment. Additionally, the potassium concentration of the KOH-loaded Y zeolite is determined using EDX analysis to confirm whether the reactivated catalysts may be employed again in the process, as shown in Figures 6, c and d. Since the concentration of K-species that connected to the active sites within the KOH/Y-zeolite catalyst did not change significantly, it can be said that the KOH/HY-zeolite catalyst is generally more suitable for such a catalytic process and can be expected to have a better catalytic performance during the reactions. In fact, it is important to ensure that within a heterogeneous catalyst, the active metal species are not significantly eroded from the solid support of the catalyst during either the reaction or reactivation treatment after the reaction. If large amounts of the active metal species, which act as a homogeneous part, leak out of the catalyst, the catalytic process advantages of the heterogeneous catalysts can be lost [46,47].

3.5 Atomic Force Microscopy (AFM) Analysis

Using an atomic force microscopy (AFM) system with a high-resolution image of the catalyst surface, the topography of the resulting catalyst is investigated. Compared to the SEM-images, the AFM-images provide additional details about the catalyst surface composition. The catalyst made with Ludox AS-40 has nano-scale characteristics with an average particle diameter of about 416 nm, according to the published literature [48,49]. The particle size histogram distribution of the as-prepared Y-zeolites is shown in Figure 7 (a) 2-dimensional image and (b) 3-dimensional image, and the entire distribution spans from 200 to 1600 nm. For 50% of the average particle sizes were in the range of less than 200 nm, and according to the AFM results, 42% of the sample particle sizes were in the range of 900 nm or smaller.

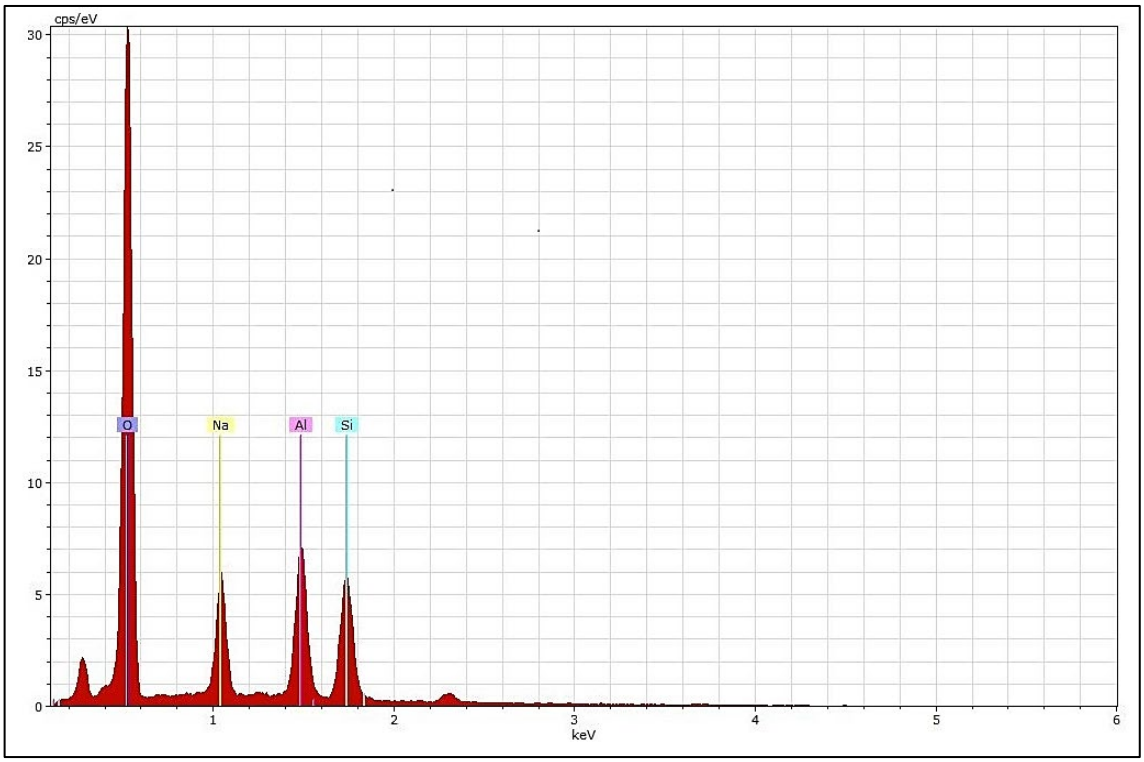

(a)

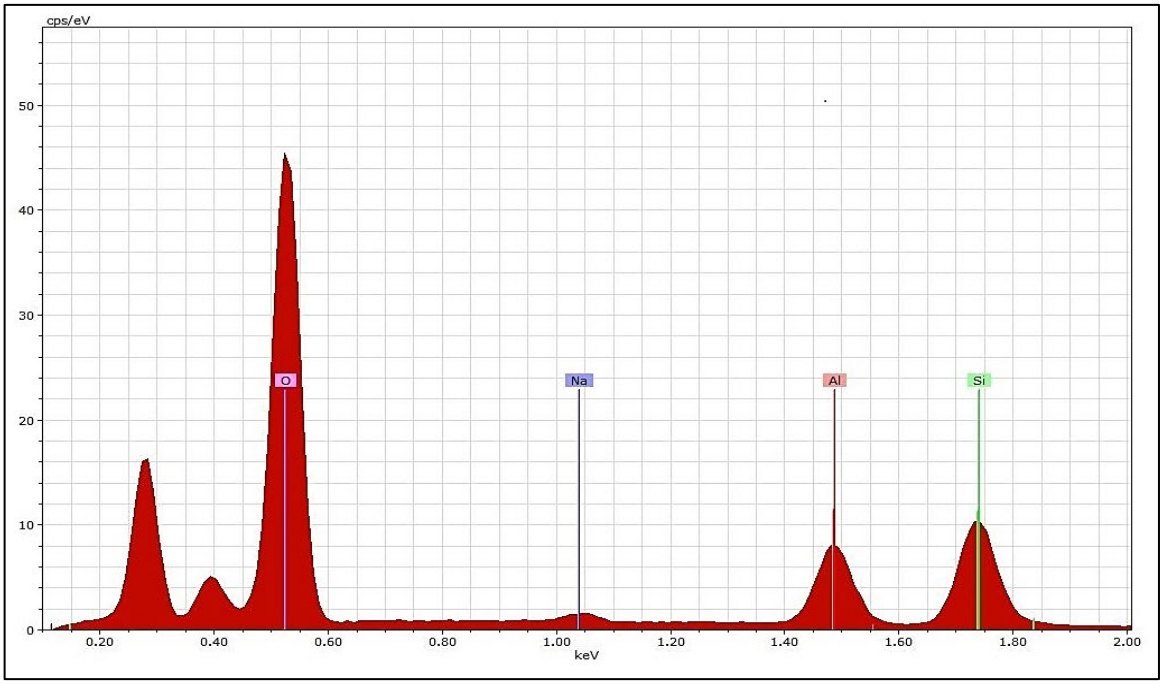

(b)

Figure 6: EDX-spectra of (a) The synthesized NaY-zeolite form, (b) NH_4-Y zeolite form, (c) KOH/HY-zeolite catalyst, and (d) The regenerated KOH/HY-zeolite catalyst

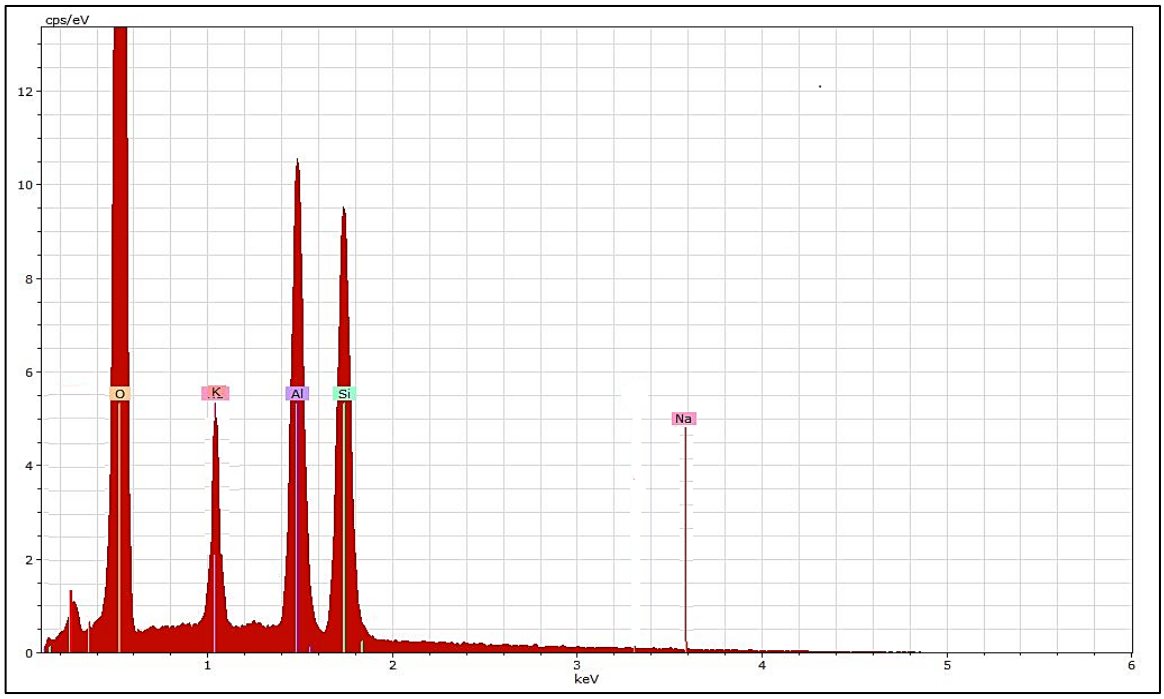

(c)

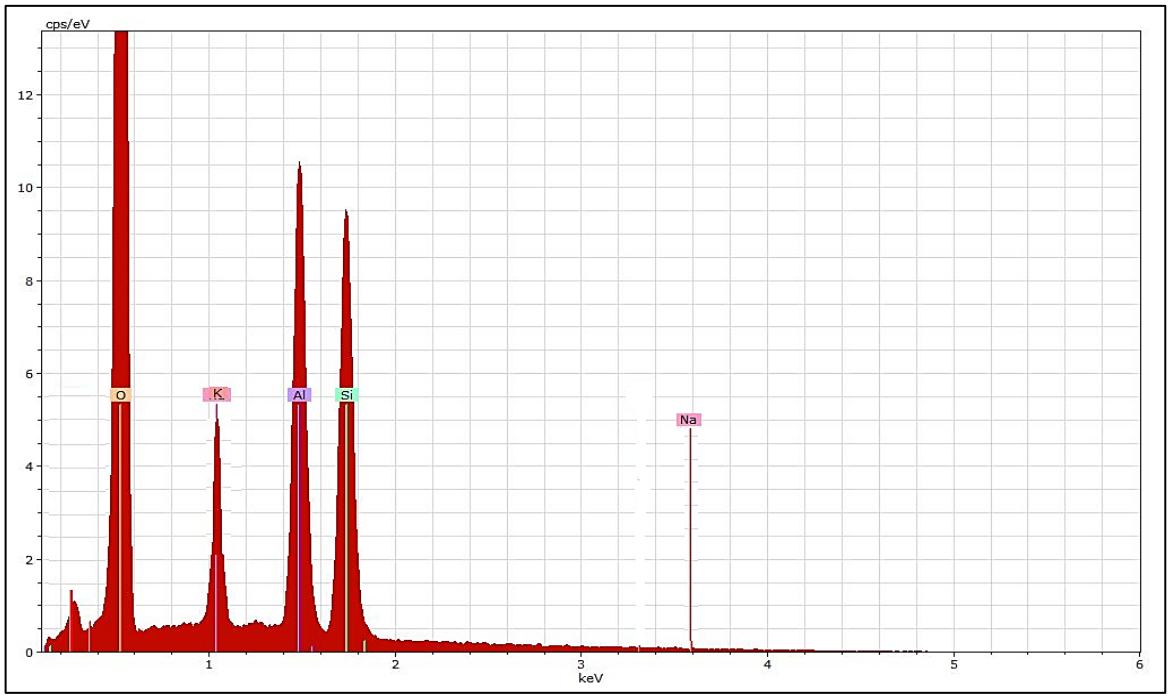

(d)

Figure 6: Continued

3.6 Fourier-Transformed Infrared Spectroscopy (FT-IR) Analysis

The infrared approach is used to evaluate the chemistry of the catalyst surface, including surface acidity. As illustrated in Figure 8, the functional groups and areas present in wave numbers between 500 and 4000 cm^{-1} are used to describe the Faujasite structure. The bands that are visible between 3472 and 3536 cm^{-1} pointed to the Al-OH-stretching band in the sodalite cage, which is made up of SiO_4 molecules and Brønsted acid protons, commonly known as the low-frequency band. The bending vibration of water molecules within the zeolite structure causes the peak at around 1636.75 cm^{-1}. At the same time, the band at about 627 cm-^{1} is attributed to internal tetrahedral symmetrical stretching. The bands in the range of 988 cm^{-1} suggest the existence of Si-O and are ascribed to external asymmetrical stretching. It is observed that the Al-band is in octahedral coordination, and Si-O-Al stretching is attributed to the absorption at around 451-468 cm^{-1}. When comparing, in light of what is stated in the literature, it is clear that all active groups within the structure of the catalyst prepared in the laboratory are identical to the results of the research publications [50,51]. In fact, it is concluded that the FTIR-spectra of the synthesized HY zeolite matched the usual absorption peaks of the commercial HY zeolite.

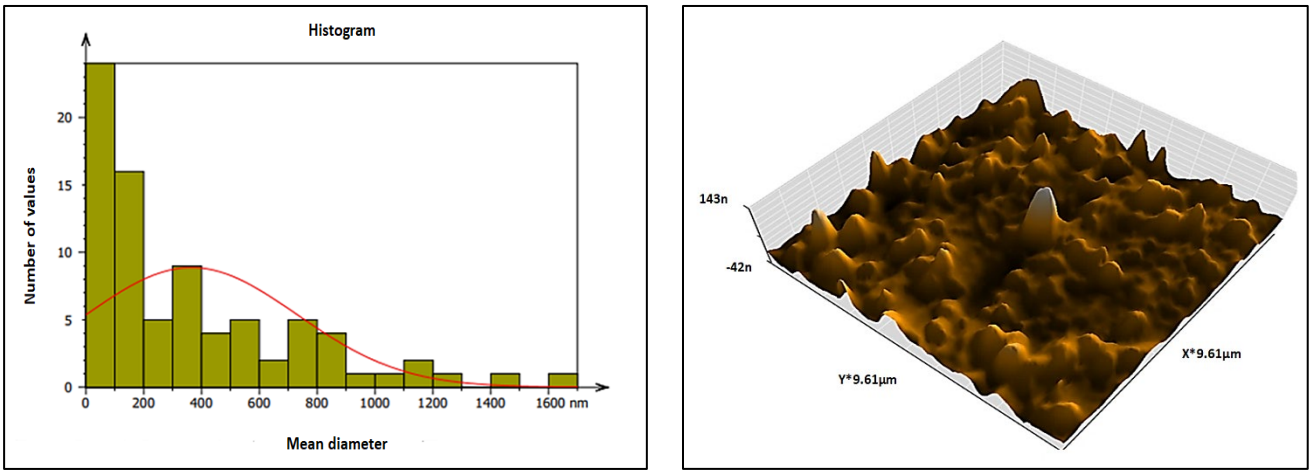

(a) 2-Dimensional image **(b) 3-Dimensional image**

Figure 7: AFM surface analysis of particle size distribution of the as-prepared Y-catalyst

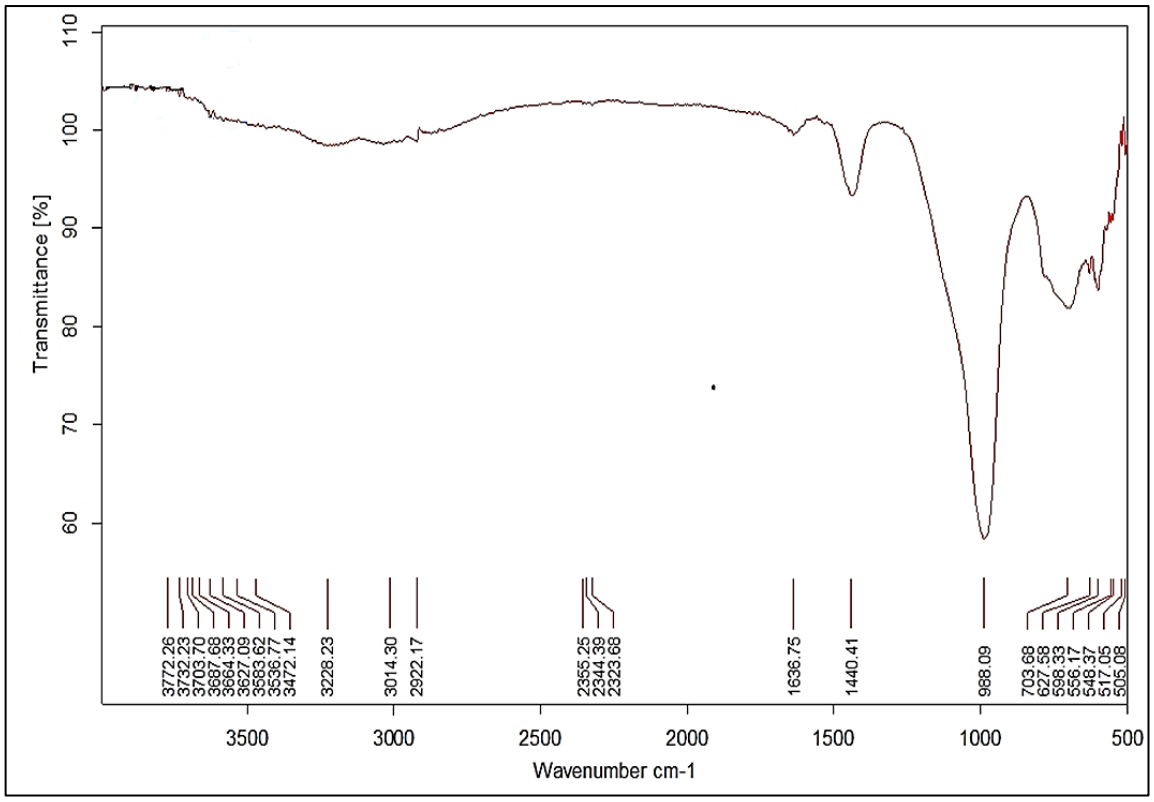

Figure 8: FTIR spectrum of the synthesized Y-zeolite

4. Effect of Reaction Conditions on Biodiesel Produced

4.1 Effect of Catalyst Particle Size

Particle size affects catalytic properties, including activity, porosity, and surface area. Figure 9, a-c, shows that when the particle size decreases from 1000 to 75 µm, the WCO conversion increases. When using a Y-zeolite catalyst with the largest particle size of 1000 µm, WCO conversion is at a minimum value. A particle size of 75µm results in maximum product conversion. The surface reaction and/or the accessible surface area of the reactant are limited by the catalyst particles. There are unequivocally greater conversions to methyl esters when active sites are available, and the reaction rate is known to increase with decreasing catalyst particle size. Moreover, compared to the reaction on the external surface, the diffusion of the reactants into the internal surface of the Y-zeolite catalyst pores takes a relatively long time. As a result, the outer surface of the catalyst is the only place where the reactant is consumed, resulting in poor conversion when using large-sized catalyst particles [52]. The catalyst is expected to have a larger surface area with a particle size of 75 µm, which increases the reaction rate and improves conversion due to the reduction of the external mass transfer barrier of the reactants into the pores of the catalyst. As mentioned earlier, in the heterogeneous catalytic process, the reaction rate is inversely proportional to the particle size of the catalyst used [53].

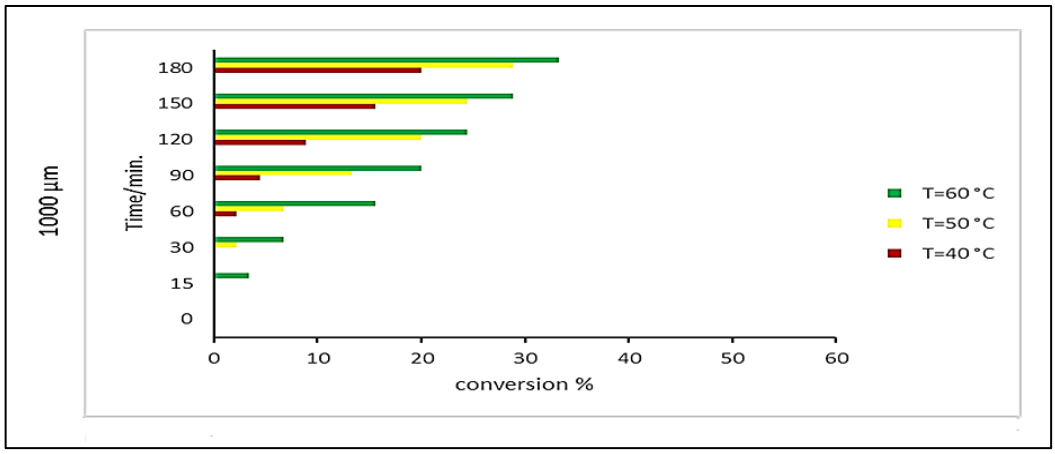

(a) Conversion of WCO as a function of reaction time at 40, 50, and 60℃ using partical size of 1000 µm

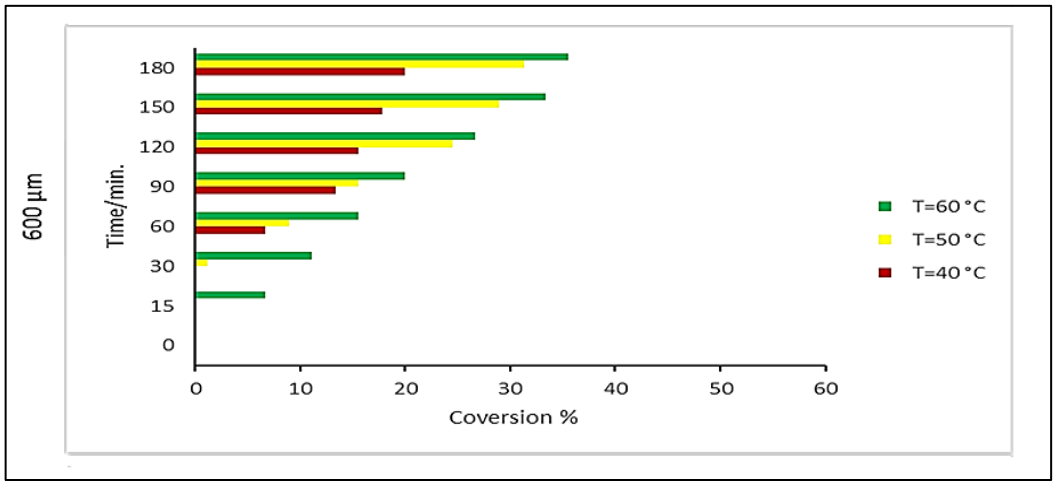

(b) Conversion of WCO as a function of reaction time at 40, 50, and 60 ℃ using partical size of 600 µm

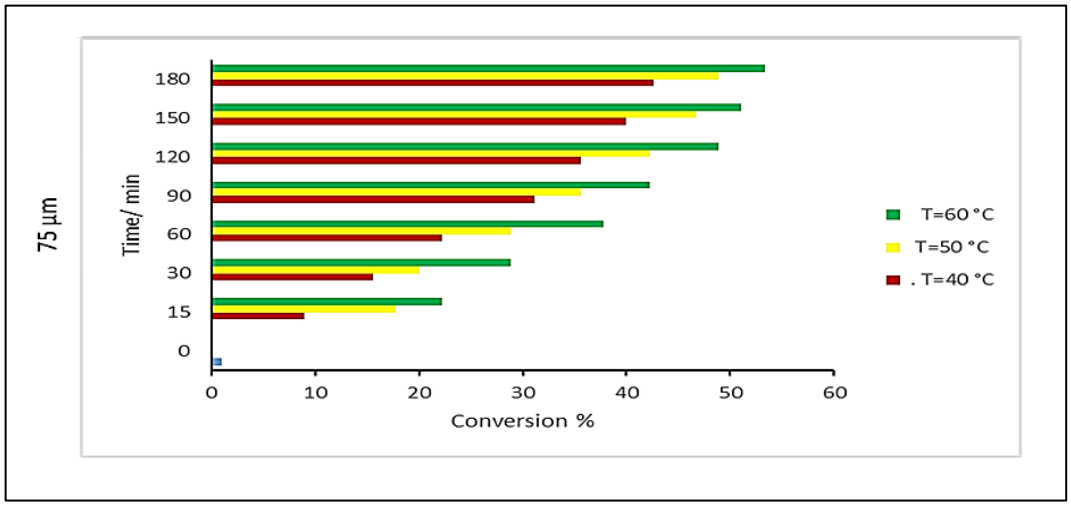

(c) Conversion of WCO as a function of reaction time at 40, 50, and 60℃ using partical size of 75 µm

Figure 9: Conversion of WCO as a function of reaction time at 40, 50 and 60℃ using various unloaded Y-zeolite catalyst particle sizes

4.2 Effect of Reaction Time and Reaction Temperature

According to Figure 9, the type of catalyst particle sizes and reaction temperature at a constant molar ratio of MeOH/Oil determine how much biodiesel is converted over time, for example, with a MeOH : Oil molar ratio of 11.5, 600 rpm stirring speed, and reaction temperatures of 40, 50, and 60℃. The largest biodiesel conversion of 53.33% was achieved within 3 h at 60℃ using a non-KOH-loaded Y-zeolite catalyst with a particle size of 75 µm. It is also observed that the biodiesel conversion increases with the reaction duration.

On the other hand, Figure 10, a-c, shows the impact of reaction temperature on biodiesel production from WCO transesterification processes. The reaction temperature had a significant effect on biodiesel yield using an unloaded Y-zeolite catalyst with a particle size of 75 µm, where the greatest yield was achieved between 40 and 60℃ on its surface. The

maximum yield of products was achieved with a reaction time of 3 h at 60°C, in other words, the longer the reaction time and the higher the temperature, the greater the yield of reaction products.

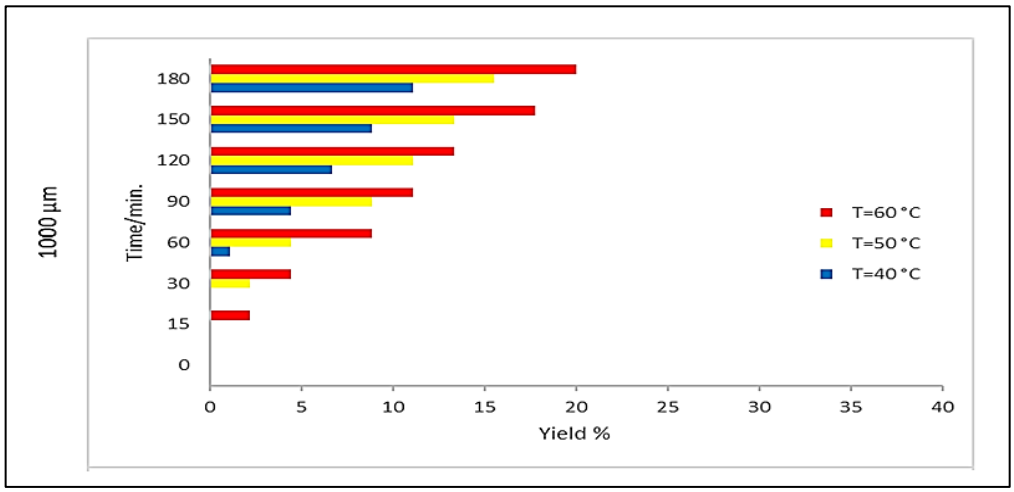

(a) Biodiesel yield as a function of reaction time at 40, 50, and 60°C using partical size of 1000 µm

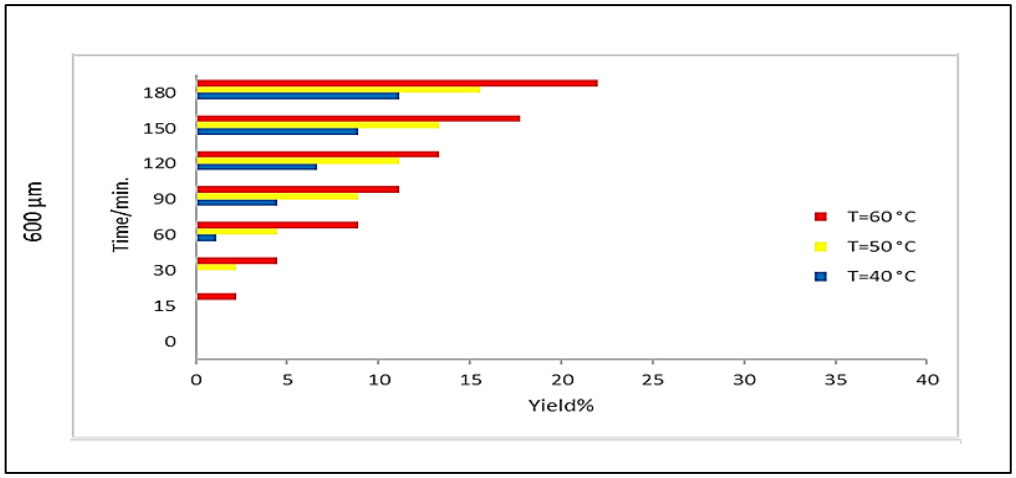

(b) Biodiesel yield as a function of reaction time at 40, 50, and 60°C using partical size of 600 µm

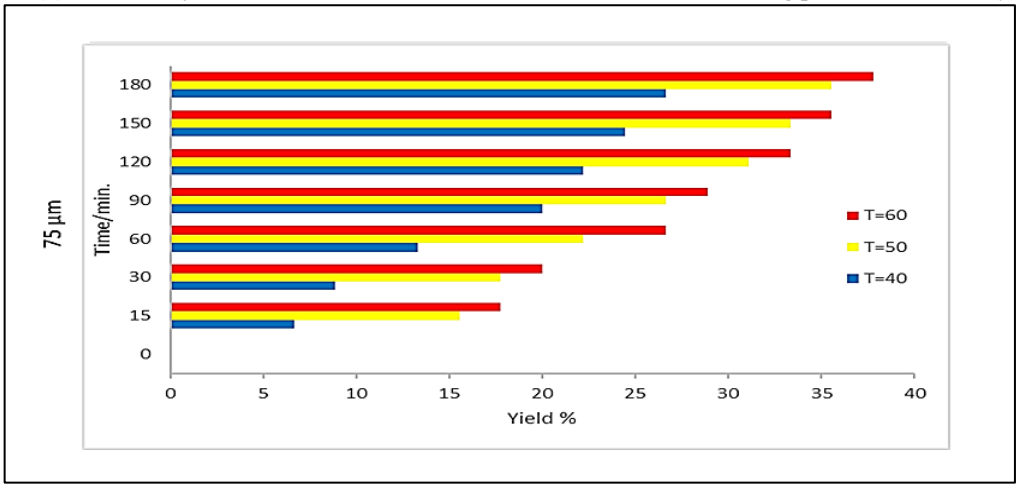

(c) Biodiesel yield as a function of reaction time at 40, 50, and 60°C using partical size of 75 µm

Figure 10: Biodiesel yield as a function of reaction time over different particle sizes of unloaded Y-zeolite catalysts at temperatures of 40, 50 and 60°C

4.3 Effect of KOH Loaded on The Catalyst Surface

The process of loading 10 wt% KOH onto a zeolite catalyst leads to the synthesis of KOH/HY zeolite catalysts, which are then used to catalyze the trans-esterification reaction using 75 µm particle size of the catalyst during 3 h, 0.5 v/v MeOH : Oil ratio (i.e. 11.5 M ratio) and 5.76 wt% Catalyst Weight : WCO ratio at 60°C. The results demonstrate that the produced biodiesel conversion increased with the reaction time, and it peaked at 2 h with the maximum conversion and the highest yield reaching 84.44 and 80%, respectively, as shown in Figure 11-a. It has been proven that extending the reaction time to 3 h leads

to a decrease in conversion and low yield, reaching 80 and 77.78%, respectively. Comparing these results with the previously reported results for the unloaded HY zeolite catalyst, it appears that the KOH/HY-fresh zeolite catalyst was affected by an increase in reaction time, which causes a decrease in its activity during the reaction, and thus a decrease in yield and conversion too. In addition, this behavior could be due to the prolongation of the reaction time, which leads to the hydrolysis of esters and more fatty acids to turn into soaps [54], and the decrease in the activity and basicity of the loaded catalyst during the process mechanism, which somewhat encouraged the esterification reactions of the free fatty acids with glycerol and consequently reducing the amount of biodiesel produced [55]. From the comparison, at the same reaction time for the homogenous catalyst KOH the biodiesel yield increases after 2 h because the soap formation is lower than the heterogenous catalyst those found in previous studies [56,57]. Furthermore, to evaluate whether the reactivated catalyst can be reused in the post-reaction by examining whether the deactivated Y-zeolite catalyst can be recycled under the same reaction conditions. Filtration and regeneration were used to separate the spent catalyst from the reaction products at the end of the reaction.

Thus, another identical process lasting 3 h at 60°C was applied using the same 75 µm particle size of 10 wt% KOH/HY-reactivated zeolite catalysts. Within a couple of hours, the diesel fuel production reached its maximum. It reduced again after another hour of reaction time, as it was seen that the yield decreased from 80 to 72%, and conversion also diminished from 84.44 to 77%, as shown in Figure 11-b. The feasibility of reusing the catalyst after its activation in the trans-esterification processes of the WCO to produce biodiesel several times has great economic benefits on the overall process in terms of reducing the cost of using new expensive catalysts. It can be concluded that the activity of the loaded KOH represents the basicity of the catalyst, and corresponds in the opposite direction to the acidity of the catalyst, which is represented by the Lewis and Brønsted acid sites within the zeolite structure. These acidic and basic sites create the optimal balance for the reaction to occur. Increasing the reaction time negatively affects the activity of these sites, which sometimes leads to an increase in the production of glycerol at the expense of a decrease in the production of biodiesel, according to the following Equation 5:

$$\begin{array}{lll} CH_2-OOC-R_1 & & R_1-COO-R' \quad CH_2-OH \\ CH-OOC-R_2+3\,R'OH & \overset{Catalyst}{\Longleftrightarrow} & R_2-COO-R'+CH-OH \\ CH_2-OOC-R_3 & & R_3-COO-R' \quad CH_2-OH \end{array} \qquad (5)$$

TGA Alcohol Alkyl-ester Biodiesel Glycerol

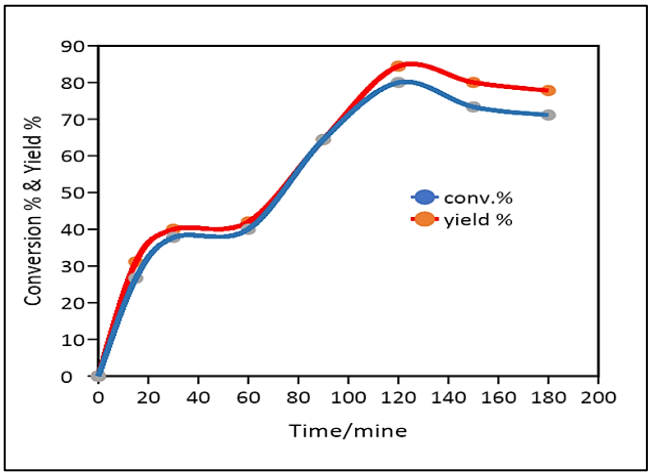

(a) 10 wt% KOH/HY-fresh zeolite catalyst

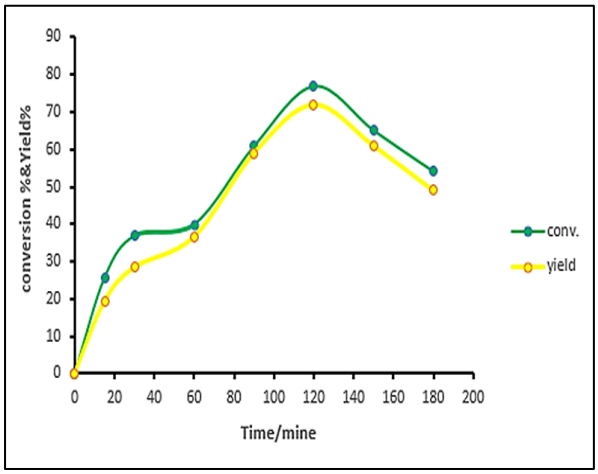

(b) 10 wt% KOH/HY-reactivated zeolite catalyst

Figure 11: Catalytic behavior over 75 µm particle size of (a) 10 wt% KOH/HY-fresh zeolite catalyst and (b) 10 wt% KOH/HY-reactivated zeolite catalyst in biodiesel production reactions for 3 h at 60°C

5. Testing Components and Properties of Waste Cooking Oil and Biodiesel

5.1 GC-MS Chromatogram Analysis

Free fatty acids (FFAs) were quantified in the sample, and the acid value (AV) of the feedstock from the remaining frying oil was 0.8 mg KOH per gram of oil. The basic catalyzed transesterification application criteria for the acid values of the feedstock are often met by the acid values of the feedstock present in this test. According to the published literature, the appropriate acid value is usually less than 1.0 mg KOH per gram of oil [58].

GC-MS chromatogram analysis of a biodiesel sample produced during the methyl esterification process by heating waste cooking oil components at temperatures of 40, 50, and 60°C for 3 h over the best HY catalyst particle size of 75 µm was used. The total fatty acid methyl ester concentration at the three temperatures mentioned above was determined to be 27.933, 37.158, and 39.303%, respectively. Tables 3 to 5 show the results of calculations for various FAME concentrations.

In addition, the accuracy of laboratory result calculations is determined by comparing the calculated laboratory yield results (i.e., the productivity) with those obtained from GC-MS for 3 h biodiesel production using the best HY catalyst (i.e., 75 µm particle size) prior to loading with 10% KOH under different temperatures (i.e., 40, 50 and 60°C). Table 6 displays the yield results obtained from the comparison, and it is clearly noted that they give good agreement, and this logically indicates the accuracy of the laboratory results calculations.

5.2 Physical and Chemical Characteristics of Biodiesel

The properties of the produced biodiesel have been measured, including kinematic viscosity, flashpoint, specific gravity, calorific value, and acid number, which are important criteria for determining the fuel efficiency produced from waste cooking oil. In fact, these measurements were made to determine the quality and the physical characteristics of the locally produced biodiesel fuel and to compare it with the standard properties of the produced diesel fuel globally. Table 7 gives an illustration of these characteristics, and the results show the great convergence between the characteristics of laboratory-produced fuels with those of globally-produced fuels.

Table 3: Calculations of various FAME concentrations at 40°C

No.	R.T. (min.)	Area	Compounds	FAME	M.Wt.
1	7.306	0.54%	$C_9H_{18}O_2$	C9:0	158.2
2	17.244	1.09%	$C_{15}H_{30}O_2$	C15:0	242.4
3	18.84	0.80%	$C_{16}H_{30}O_2$	C16:1	254.5
4	20.034, 23.192, 24.938,	3.99%, 2.36%, 0.72%	$C_{19}H_{36}O_2$	C19:1	296.5
5	20.416	11.943%	$C_{17}H_{34}O_2$	C17:0	270.5
6	21.361	0.72%	$C_{17}H_{32}O_2$	C17:1	268.5
7	21.698	0.24%	$C_{18}H_{34}O_2$	C18:1	282.5
8	23.371, 23.741	0.63%, 0.66%	$C_{19}H_{34}O_2$	C19:2	294.5
9	23.542	0.55%	$C_{21}H_{36}O_2$	C21:3	320.5
10	24.517	0.62%	$C_{21}H_{32}O_2$	C21:5	316.5
11	24.701	0.54%	$C_{16}H_{26}O_3$	C16:3	266.4
12	25.206	0.47%	$C_{21}H_{42}O_2$	C21:0	326.6
13	25.696	0.50%	$C_{54}H_{110}$	-	759.5
14	26.468	0.61%	$C_{25}H_{42}O_2$	C25:4	374.6
15	26.617	0.16%	$C_{22}H_{34}O_2$	C22:5	330.6
16	27.266,	0.79%	$C_{23}H_{46}O_2$	C23:0	354.6
17	29.21	0.27% 27.933	$C_{25}H_{50}O_2$	C25:0	382.7

Table 4: Calculations of various FAME concentrations at 50°C

No.	R.T. (min.)	% (Area)	Compounds	FAME	M.Wt.
1	7.287	0.28%	$C_9H_{18}O_2$	C9:0	158.2
2	17.2, 21.063, 21.272	1.65%, 0.26%, 0.85%	$C_{15}H_{30}O_2$	C15:0	242.4
3	18.354	0.18%	$C_{19}H_{32}O_2$	C19:3	292.5
4	18.503, 19.959, 24.878	0.12%, 3.49%, 0.88%	$C_{19}H_{36}O_2$	C19:1	296.5
5	18.768	0.84%	$C_{16}H_{30}O_2$	C16:1	254.5
6	19.717	0.69%	$C_{17}H_{28}O_2$	C17:3	264.4
7	20.338	9.26%	$C_{17}H_{34}O_2$	C17:0	270.5
8	21.6	0.39%	$C_{18}H_{36}O_2$	C18:0	284.5
9	22.623, 22.961, 23.641	11.108%, 2.38%, 0.20%	$C_{19}H_{34}O_2$	C19:2	294.5
10	23.077	2.15%	$C_{19}H_{38}O_2$	C19:0	298.5
11	23.412	0.15%	$C_{20}H_{32}O_2$	C20:4	304.5
12	23.784	0.12%	$C_{20}H_{38}O_2$	C20:1	310.5
13	24.447	0.78%	$C_{21}H_{32}O_2$	C21:5	316.5
14	24.649	0.14%	$C_{18}H_{34}O_3$	C18:1	298.5
15	25.162	0.47%	$C_{21}H_{42}O_2$	C21:0	326.5
16	26.434	0.10%	$C_{23}H_{34}O_2$	C23:6	342.5
17	27.241	0.55%	$C_{22}H_{44}O_2$	C22:0	340.6
18	29.195	0.12% 37.158	$C_{25}H_{50}O_2$	C25:0	382.7

Table 5: Calculations of various FAME concentrations at 60°C

No.	R.T. (min.)	% (Area)	Compounds	FAME	M.Wt.
1	7.292	0.15%	$C_9H_{18}O_2$	C9:0	158.2
2	13.978	0.50%	$C_{13}H_{26}O_2$	C13:0	214.3
3	17.189	0.55%	$C_{15}H_{30}O_2$	15:0	242.4
4	18.351	0.11%	$C_8H1_0O_2$	C8:3	138.2
5	18.499, 23.753, 24.862	0.12%, 0.08%, 0.35%	$C_{19}H_{36}O_2$	C19:1	296.5
6	18.759	0.67%	$C_{16}H_{30}O_2$	C16:1	254.5
7	19.702	0.15%	$C_{19}H_{32}O_2$	C19:3	292.5
8	19.941	1.37%	$C_{17}H_{32}O_2$	C17:1	268.4
9	20.305	9.16%	$C_{17}H_{34}O_2$	C17:0	270
10	21.078	0.13%	$C_{18}H_{36}O_2$	C18:0	284.5
11	21.243	0.49%			
12	21.578	0.13%	$C_{17}H_{34}O_2$	C17:0	270
13	22.674	20.943%	$C_{18}H_{32}O_2$	C18:2	280.4
14	22.978	2.45%	$C_{19}H_{38}O_2$	C19:0	298.5
15	23.158, 23.606	0.26%, 0.16%	$C_{18}H_{32}O_2$	C18:2	280.4
16	23.358	0.15%	$C_{20}H_{32}O_2$	C20:4	304.5
17	24.42, 26.576	0.47%, 0.15%	$C_{21}H_{32}O_2$	C21:4	216.5
18	25.144	0.27%	$C_{21}H_{42}O_2$	C21:0	326.5
19	26.428	0.18%	$C_{23}H_{34}O_2$	C23:6	342.5
20	27.229	0.31%	$C_{22}H_{44}O_2$	C22:0	340.6
		39.303			

Table 6: Comparison results for biodiesel yield

Temperature (°C)	40	50	60
Laboratory results Yield (%)	26.67	35.56	37.78
GC-MS results Yield (%)	27.933	37.158	39.303

Table 7: Characteristics of the biodiesel produced

Properties	Units	Test method	Min. limit	Max. limit	The value of biodiesel produced in the current study
Kinematic viscosity at 40°C	mm^2/sec.	STM D-6751 [59]	1.9	6	7.543, ASTM D-7042
Kinematic viscosity at 100°C	mm^2/sec.				2.6441, ASTM D-7042
Specific gravity at 15°C		EN-BD: EN 14214 [60]	0.86	0.9	0.9009, ASTM D-7042
Flash point	°C	STM D-6751 [59]	55	130	165, ASTM D-6450
Calorific value	MJ/kg	EN14213 [61]		35	38.122, ASTM D-240
Acid value (AV)	mg KOH/ g oil	STM D-6751 [59]	0.5	0.8	0.5

6. Conclusion

The study concluded that the utilization of laboratory-prepared HY-zeolite catalyst loaded with 10% KOH using the impregnation method enhances its activity in catalyzing reactions, particularly in the transesterification of waste cooking oil. This resulted in a conversion rate of 84.44% and a yield of 80%. The primary focus of this research was to analyze the impact of catalyst particle size on the reaction pathways. The findings indicated that smaller catalyst particle sizes, such as 75 µm, accelerated the reaction rate, thereby increasing overall productivity. The study also optimized the reaction conditions, including temperature and time, and revealed that higher reaction temperatures and/or longer reaction times positively affected the yields of reaction products using the non-KOH-loaded catalyst. Although the activity of the catalyst was improved by loading it with 10% KOH, long reaction times of more than two hours subsequently caused a decrease in catalytic efficiency. Optimal conditions for the highest biodiesel production were determined as a 0.5 v/v MeOH/Oil ratio (equivalent to an 11.5 M ratio) and a 5.76% Catalyst Weight : WCO ratio at 60°C with an agitation speed of 800 rpm. A comparison between the laboratory-calculated compounds and biodiesel yield and the results obtained from GC-MS tests demonstrated reasonable agreement. Furthermore, an examination of the physical properties of biodiesel produced from spent cooking oils was carried out, and a comparison was made against the properties of standard-fuel production procedures. The results of this comparison confirmed the satisfactory quality of the produced biodiesel fuel, which can be effectively employed as an alternative fuel source. Importantly, the study deduced that the use of a base-loaded heterogeneous catalyst, particularly KOH at a concentration not exceeding 10%, eliminates the requirement for high-cost, high-percentage homogeneous catalysts that are challenging to separate and reuse. In practice, the heterogeneous solid catalyst was successfully extracted from the reaction products, reactivated, and reutilized in post-reactions to achieve biodiesel production with acceptable conversion and yield. This contributes to a reduction in the overall economic cost of the process, as demonstrated by this study.

Acknowledgment

The authors are grateful to the Department of Chemical Engineering, University of Technology in Baghdad - Iraq, for providing laboratories and facilities and completing all technical tests required for the experiments.

Author contributions

Conceptualization, H. Abdul-Kader. Z. Shakor. B. Al-Zaidi. Sh. Al-Humairi. M. alihu; methodology, H. Abdul-Kader; formal analysis, Z. Shakor; investigation, Sh. Al-Humairi; resources, Z. Shakor. B. Al-Zaidi, and Sh. Al-Humairi; data curation, B. Al-Zaidi; writing—original draft preparation, Z. Shakor. and B. Al-Zaidi; writing—review and editing, Sh. Al-Humairi. and B. Al-Zaidi; supervision, H. Abdul-Kader. All authors have read and agreed to the published version of the manuscript.

Funding

This research received no specific grant from any funding agency in the public, commercial, or not-for-profit sectors.

Data availability statement

The data that support the findings of this study are available on request from the corresponding author.

Conflicts of interest

The authors declare that there is no conflict of interest.

References

[1] N. Mansir, Y. H. T.Yap, U. Rashid, I. M. Lokman, Investigation of heterogeneous solid acid catalyst performance on low grade feedstocks for biodiesel production: A review, Energy. Convers. Manag., 141(2017)171–182.

[2] K. F. Yee, J. Kansedo, K. T. Lee, Biodiesel production from palm oil via heterogeneous transesterification: optimization study, Chem. Eng. Commun., 197 (2010) 1597–1611. https://doi.org/10.1080/00986445.2010.500156

[3] J. Kansedo, K. T. Lee, S. Bhatia, Biodiesel production from palm oil via heterogeneous transesterification, Biomass. Bioenergy., 33 (2009) 271–276. https://doi.org/10.1016/j.biombioe.2008.05.011

[4] S. T. Al-Humairi, J. G. M. Lee, A. P. Harvey, Direct and rapid production of biodiesel from algae foamate using a homogeneous base catalyst as part of an intensified process, Energy .Convers. Manag., 16 (2022) 100284. https://doi.org/10.1016/j.ecmx.2022.100284

[5] M. Y. Koh , T. I. Mohd, Ghazi, A review of biodiesel production from Jatropha curcas L. oil, Renew. Sust. Energ. Rev., 15 (2011) 2240–2251. https://doi.org/10.1016/j.rser.2011.02.013

[6] M. N. Nabi, M. M. Rahman, M. S. Akhter, Biodiesel from cotton seed oil and its effect on engine performance and exhaust emissions, Appl. Therm. Eng., 29 (2009) 2265–2270. https://doi.org/10.1016/j.applthermaleng.2008.11.009

[7] X. Meng, G. Chen, Y. Wang, Biodiesel production from waste cooking oil via alkali catalyst and its engine test, Fuel Process. Technol., 89 (2008) 851–857. https://doi.org/10.1016/j.fuproc.2008.02.006

[8] H. N. Bhatti, M. A. Hanif, M. Qasim, Biodiesel production from waste tallow, Fuel, 87(2008) 2961–2966. https://doi.org/10.1016/j.fuel.2008.04.016

[9] P. Cao, M. A. Dubé, A. Y. Tremblay, High-purity fatty acid methyl ester production from canola, soybean, palm, and yellow grease lipids by means of a membrane reactor, Biomass . Bioenergy ., 32 (2008) 1028–1036. https://doi.org/10.1016/j.biombioe.2008.01.020

[10] H.Y. Shin, S. H. Lee, J. H. Ryu, S. Y. Bae, Biodiesel production from waste lard using supercritical methanol, J. Supercrit. Fluids, 61 (2012)134–138. https://doi.org/10.1016/j.supflu.2011.09.009

[11] M. Gürü, A. Koca, Ö. Can, C. Çınar, F. Şahin, Biodiesel production from waste chicken fat based sources and evaluation with Mg based additive in a diesel engine, Renew. Energy., 35 (2010) 637–643. https://doi.org/10.1016/j.renene.2009.08.011

[12] E. Alptekin , M. Canakci, Optimization of pretreatment reaction for methyl ester production from chicken fat, Fuel, 89 (2010) 4035–4039. https://doi.org/10.1016/j.fuel.2010.04.031

[13] A. Gaurav, S. Dumas, C. T. Q. Mai, F. T. T. Ng, A kinetic model for a single step biodiesel production from a high free fatty acid (FFA) biodiesel feedstock over a solid heteropolyacid catalyst, Green. Energy. Environ., 4 (2019)328–341. https://doi.org/10.1016/j.gee.2019.03.004

[14] S. Nisar, M. A. Hanif, U. Rashid, A. Hanif, M. N. Akhtar, C. Ngamcharussrivichai, Trends in widely used catalysts for fatty acid methyl esters (Fame) production: A review, Catal., 11 (2021) 1085 . https://doi.org/10.3390/catal11091085

[15] E. Leclercq, A. Finiels, C. Moreau, Transesterification of rapeseed oil in the presence of basic zeolites and related solid catalysts, J. Amer. Oil Chem. Soc., 78 (2001)1161–1165. https://doi.org/10.1007/s11746-001-0406-9

[16] T. Ebiura, T. Echizen, A. Ishikawa, K. Murai, T. Baba, Selective transesterification of triolein with methanol to methyl oleate and glycerol using alumina loaded with alkali metal salt as a solid-base catalyst, Appl. Catal. A Gen., 283 (2005) 111–116. https://doi.org/10.1016/j.apcata.2004.12.041

[17] D. Qasim, Y. I. Abdul-Aziz, Z. T. Alismaeel, Biodiesel from fresh and waste sunflower oil using calcium oxide catalyst synthesized from local limestone, Res. J. Chem. Environ., 23 (2019)111–119.

[18] G. J. Suppes, M. A. Dasari, E. J. Doskocil, P. J. Mankidy, M. J. Goff, Transesterification of soybean oil with zeolite and metal catalysts, Appl. Catal. A Gen., 257 (2004) 213–223. https://doi.org/10.1016/j.apcata.2003.07.010

[19] D. G. Cantrell, L. J. Gillie, A. F. Lee, K. Wilson, Structure-reactivity correlations in MgAl hydrotalcite catalysts for biodiesel synthesis, Appl. Catal. A Gen., 287 (2005) 183–190. https://doi.org/10.1016/j.apcata.2005.03.027

[20] W. Xie, H. Peng, L. Chen, Calcined Mg–Al hydrotalcites as solid base catalysts for methanolysis of soybean oil, J. Mol .Catal. A Chem., 246 (2006) 24–32. https://doi.org/10.1016/j.molcata.2005.10.008

[21] N. Al-Jammal, Z. Al-Hamamre, M. Alnaief, Manufacturing of zeolite based catalyst from zeolite tuft for biodiesel production from waste sunflower oil, Renew. Energy., 93 (2016) 449–459. https://doi.org/10.1016/j.renene.2016.03.018

[22] L. Tosheva, A. Brockbank, B. Mihailova, J. Sutula, J. Ludwig, H. Potgietera J.Verrana , Micron-and nanosized FAU-type zeolites from fly ash for antibacterial applications, J. Mater. Chem., 22 (2012)16897–16905. https://doi.org/10.1039/C2JM33180B

[23] A. S. Abbas , R. N. Abbas, Preparation and characterization of NaY zeolite for biodiesel production, J. Chem. Pet. Eng., 16 (2015) 19–29. https://doi.org/10.31699/IJCPE.2015.2.3

[24] C. Belviso, L. C. Giannossa, F. J. Huertas, A. Lettino, A. Mangone, S. Fiore, Synthesis of zeolites at low temperatures in fly ash-kaolinite mixtures, Microporous Mesoporous Mater., 212 (2015) 35–47.

[25] A. M. Doyle, Z. T. Alismaeel, T. M. Albayati, A. S. Abbas, High purity FAU-type zeolite catalysts from shale rock for biodiesel production, Fuel, 199 (2017) 394–402.

[26] W. Xie, X. Huang, H. Li, Soybean oil methyl esters preparation using NaX zeolites loaded with KOH as a heterogeneous catalyst, Bioresour. Technol., 98 (2007) 936–939. https://doi.org/10.1016/j.biortech.2006.04.003

[27] M. J. Ramos, A. Casas, L. Rodríguez, R. Romero, Á. Pérez, Transesterification of sunflower oil over zeolites using different metal loading: A case of leaching and agglomeration studies, Appl. Catal. A Gen., 346 (2008)79–85. https://doi.org/10.1016/j.apcata.2008.05.008

[28] H. Wu, J. Zhang, Q. Wei, J. Zheng, J. Zhang, Transesterification of soybean oil to biodiesel using zeolite supported CaO as strong base catalysts, Fuel Process. Technol., 109 (2013)13–18. https://doi.org/10.1016/j.fuproc.2012.09.032

[29] N. Al-Jammal, Z. Al-Hamamre, M. Alnaief, Manufacturing of zeolite based catalyst from zeolite tuft for biodiesel production from waste sunflower oil, Renew. Energy., 93 (2016) 449–459 . https://doi.org/10.1016/j.renene.2016.03.018

[30] M. C. Manique, L. V. Lacerda, A. K. Alves, C. P. Bergmann, Biodiesel production using coal fly ash-derived sodalite as a heterogeneous catalyst, Fuel, 190 (2017) 268–273.

[31] A. P. S. Dias, J. Puna, M. J. N. Correia, I. Nogueira, J. Gomes, J. Bordado, Effect of the oil acidity on the methanolysis performances of lime catalyst biodiesel from waste frying oils (WFO), Fuel Process. Technol., 116 (2013) 94–100. https://doi.org/10.1016/j.fuproc.2013.05.002

[32] V. Meynen, P. Cool, E. F. Vansant, Verified syntheses of mesoporous materials, Microporous. Mesoporous. Mater. ., 125 (2009)170–223. https://doi.org/10.1016/j.micromeso.2009.03.046

[33] C. S. Cundy . P. A. Cox, The hydrothermal synthesis of zeolites: Precursors, intermediates and reaction mechanism, Microporous mesoporous Mater., 82 (2005) 1–78. https://doi.org/10.1016/j.micromeso.2005.02.016

[34] B. Y. S. Al-Zaidi, The effect of modification techniques on the performance of zeolite-Y catalysts in hydrocarbon cracking reactions, The University of Manchester (United Kingdom), 2011.

[35] H. Robson, Verified synthesis of zeolitic materials. Gulf Professional Publishing, 2001.

[36] E. Lotero, Y. Liu, D. E. Lopez, K. Suwannakarn, D. A. Bruce, J. G. Goodwin, Synthesis of biodiesel via acid catalysis, Ind. Eng. Chem. Res., 44 (2005) 5353–5363. https://doi.org/10.1021/ie049157g

[37] Z. Al-Hamamre, S. Foerster, F. Hartmann, M. Kröger, M. Kaltschmitt, Oil extracted from spent coffee grounds as a renewable source for fatty acid methyl ester manufacturing, Fuel, 96 (2012) 70–76. https://doi.org/10.1016/j.fuel.2012.01.023

[38] C. Baerlocher, L. B. McCusker, D. H. Olson, Atlas of zeolite framework types. Elsevier, 2007.

[39] M. M. J. Treacy , J. B. Higgins, Collection of simulated XRD powder patterns for zeolites fifth (5th) revised. Elsevier, 2007. https://doi.org/10.1016/B978-0-444-53067-7.X5470-7

[40] X. Zhang, M. Lu, M. A. M. Idrus, C. Crombie, V. Jegatheesan, Performance of precipitation and electrocoagulation as pretreatment of silica removal in brackish water and seawater, Process .Saf. Environ. Prot., 126 (2019) 18–24. https://doi.org/10.1016/j.psep.2019.03.024

[41] Y. H. Khalaf, B. Y. Sherhan Al-Zaidi, Z. M. Shakour, Experimental and Kinetic Study of the Effect of using Zr-and Pt-loaded Metals on Y-zeolite-based Catalyst to Improve the Products of n-heptane Hydroisomerization Reactions, Orbital, 14 (2022) 153–167. https://doi.org/10.17807/orbital.v14i3.17429

[42] R. Y. Ghazal , T. A. Younus, Preparation and Studying of Zeolite with Catalytic Properties From Silica and Bauxite Ores Local, J. Educ. Sci., 30 (2021) 103–116 . https://doi.org/1033899/EDUSJ.2020.127990.1104

[43] M. Nsaif, A. Abdulhaq, A. Farhan, S. Neamat, Catalytic Cracking of Heptane using prepared zeolite, J. Asian .Sci. Res., 2 (2012) 927–948.

[44] A. H. Matti , K. M. Surchi, Comparison the properties of zeolite NaY synthesized by different procedures, Int. J. Innov. Res. Sci. Eng. Technol., 3 (2014) 13333–13342.

[45] M. J. B. Souza, A. O. S. Silva, V. J. Fernandes Jr, A. S. Araujo, Catalytic cracking of C5+ gasoline over HY zeolite, React. Kinet. Catal. Lett., 79 (2003) 257–262. https://doi.org/10.1023/A:1024530017369

[46] C. S. MacLeod, A. P. Harvey, A. F. Lee, K. Wilson, Evaluation of the activity and stability of alkali-doped metal oxide catalysts for application to an intensified method of biodiesel production, Chem. Eng. J., 135 (2008) 63–70. https://doi.org/10.1016/j.cej.2007.04.014

[47] D. M. Alonso, R. Mariscal, R. Moreno-Tost, M. D. Z. Poves, M. L. Granados, Potassium leaching during triglyceride transesterification using K/γ-Al2O3 catalysts, Catal. Commun., 8 (2007) 2074–2080. https://doi.org/10.1016/j.catcom.2007.04.003

[48] J. M. Kim , R. Ryoo, Synthesis of MCM-48 single crystals, Chem. Commun., 2 (1998) 259 –260. https://doi.org/10.1039/A707677K

[49] X. Querol , Synthesis of zeolites from coal fly ash: an overview, Int. J. coal Geol., 50 (2002) 413–423. https://doi.org/10.1016/S0166-5162(02)00124-6

[50] R. Sadeghbeigi, Fluid catalytic cracking handbook: An expert guide to the practical operation, design, and optimization of FCC units. Butterworth-Heinemann, 2020.

[51] Y. P. Peña, W. Rondón, Linde type a zeolite and type Y faujasite as a solid-phase for lead, cadmium, nickel and cobalt preconcentration and determination using a flow injection system coupled to flame atomic absorption spectrometry, Am. J. Anal. Chem., 4 (2013) 387-397. https://doi.org/10.4236/ajac.2013.48049

[52] L.C. Meher, D. V. Sagar, S.N. Naik, Technical aspects of biodiesel production by transesterification—a review, Renew. Sust. Energ. Rev., 10 (2006) 248-268. https://doi.org/10.1016/j.rser.2004.09.002

[53] H. S. Fogler, Elements of chemical reaction engineering. Pearson Boston, 2020.

[54] B. B. Uzun, M. Kiliç, N. Özbay, A. E. Pütün, E. Pütün , Biodiesel production from waste frying oils: Optimization of reaction parameters and determination of fuel properties, Energy., 44 (2012) 347–351. https://doi.org/10.1016/j.%20energy.2012.06.024

[55] M. Kouzu, T. Kasuno, M. Tajika, Y. Sugimoto, S. Yamanaka, J. Hidaka, Calcium oxide as a solid base catalyst for transesterification of soybean oil and its application to biodiesel roduction, Fuel, 87 (2008) 2798–2806. https://doi.org/10.1016/j.fuel.2007.10.019

[56] M. O. Daramola, K. Mtshali, L. Senokoane, O. M. Fayemiwo, Influence of operating variables on the transesterification of waste cooking oil to biodiesel over sodium silicate catalyst: A statistical approach, J. Taibah .Univ. Sci., 10 (2016) 675–684. https://doi.org/10.1016/j.jtusci.2015.07.008

[57] O. Ogunkunle, O. O. Oniya, A. O. Adebayo, Yield response of biodiesel production from heterogeneous and homogeneous catalysis of milk bush seed (Thevetia peruviana) oil, Energy .Policy. Res., 4 (2017) 21–28. https://doi.org/10.1080/23815639.2017.1319772

[58] F. Jalal, P. S. Ilavarasi, L. R. Miranda, Fatty methyl esters from vegetable oils for use as a diesel fuel, IEEE Conf. Clean. Energy. Technol., (2011) 125–128. https://doi.org/10.1109/CET.2011.6041472

[59] C. ASTM, 150: The American Society for Testing Materials Standard Specification for Portland Cement, West Conshohocken (PA), USA, 2002.

[60] E. N. DIN, 590: 2014-04-Automotive fuels-Diesel-Requirements and test methods, Ger. version EN, 590 (2013).

[61] J. Á. León Valdez, Evaluación del acoplamiento de energía térmica solar para la producción de biodiesel a partir de aceite vegetal residual, 2017.